

On the role of large-scale structures in wall turbulence

Ivan Marusic^{a)}

Department of Aerospace Engineering and Mechanics, University of Minnesota, Minneapolis, Minnesota 55455

(Received 7 June 2000; accepted 1 December 2000)

Recent experimental and computational studies by Adrian and co-workers, such as Adrian *et al.* [J. Fluid Mech. **422**, 1 (2000)] and Zhou *et al.* [J. Fluid Mech. **387**, 353 (1999)], have proposed that a dominant structure in wall turbulence is the organization of hairpin vortices in spatially correlated packets or trains of vortices. In this study this scenario is investigated using the attached eddy model of Perry and Marusic [J. Fluid Mech. **298**, 361 (1995)] by calculating structure angles, two-point velocity correlations and autocorrelations and comparing them to experimental measurements across a zero-pressure-gradient turbulent boundary layer. The results support the conclusion that spatially coherent packets are a statistically significant structure for Reynolds stresses and transport processes in the logarithmic region of the flow. © 2001 American Institute of Physics.
[DOI: 10.1063/1.1343480]

I. INTRODUCTION

A substantial amount of evidence has been presented in the literature supporting the existence of hairpin or horseshoe-type coherent structures in turbulent boundary layer flows, in the region above the viscous buffer zone. See, for example, Ref. 1, the review by Robinson² and the articles in Ref. 3. This evidence comes from experimental flow visualization using dye, smoke or other passive markers, and more recently from numerical datasets using vortex feature-extraction schemes. With the large number of studies have also come various labels and descriptions to identify different variations of these structures. In this article, no distinction between different variations of hairpin-type vortices is considered, for example, symmetric versus asymmetric, but rather the concern will be on shapes which are found to be statistically representative on average (in the sense of Townsend⁴). Also, no distinction is made between hairpin or horseshoe shapes and therefore only the term hairpin will be used.

Perry and Chong⁵ and Perry, Henbest and Chong⁶ were the first to use the hairpin vortex shape as the representative eddy in a kinematic model for wall turbulence. The model is based on Townsend's attached eddy hypothesis^{7,4} and considers an assemblage of eddies with a range of length scales with varying population densities per eddy length scale. The eddies are attached in the sense that their characteristic lengths are proportional to the distance at which the eddy is located from, or extends above, the wall. Perry and Marusic⁸ and Marusic and Perry⁹ later refined and extended the model to compute second order statistics, including kinetic energy spectra. Good quantitative agreement was shown for components of the Reynolds stress tensor given the experimental mean velocity flow field for a range of different studies.

One of the main underlying assumptions in the attached

eddy modeling work has been that the attached eddies are randomly distributed in the plane of the wall and therefore are uncorrelated with each other. Recent studies by Adrian and co-workers suggest that this assumption is not valid, and provide evidence suggesting that the hairpin vortices are spatially aligned in the streamwise direction, forming correlated packets or trains of vortices. In Refs. 10 and 11, it is pointed out that such a correlation leads to Reynolds stresses being enhanced by the cooperative transfer of momentum between the hairpins, which are not included in the Perry and Marusic model. The evidence for spatial coherence between individual hairpins has come from both experimental^{10,12,13} and numerical studies.¹⁴⁻¹⁶ In the study of Zhou *et al.*,¹⁴ direct numerical simulation (DNS) was used to observe the evolution of a single hairpin vortex structure embedded into the mean flow field of a low Reynolds number ($Re_\tau=180$) turbulent channel flow. Here $Re_\tau=\delta_c U_\tau/\nu$ is the Karman number where δ_c is either boundary layer thickness or channel half-width, U_τ is wall-shear velocity, and ν is kinematic viscosity. Zhou *et al.* found that provided the initial vortex had sufficiently high circulation in its core, then it would spawn other hairpin vortices which would consequently propagate together as a coherent packet of structures. Similar generation processes have been reported by Smith *et al.*¹⁷ In another numerical study, Liu and Adrian¹⁶ performed a DNS of channel flow at $Re_\tau=300$ and reported the frequent appearance of packets of hairpin vortices with lengths of approximately $3-7\delta_c$. The computational domain was $12.7\delta_c$ in the streamwise direction. Experimentally, Adrian, Meinhardt and Tomkins¹⁰ studied a zero-pressure-gradient boundary layer over a Reynolds number range of $355 < Re_\tau < 2000$ using high resolution PIV (particle image velocimetry). (This corresponds to a range of Reynolds number based on momentum thickness of $930 < R_\theta < 6845$.) They concluded that the packets appear regularly in the near-wall region and the logarithmic region of the flow and extend up to the middle of the boundary layer. Packets containing up to ten hairpin vortices

^{a)}Electronic mail: marusic@aem.umn.edu

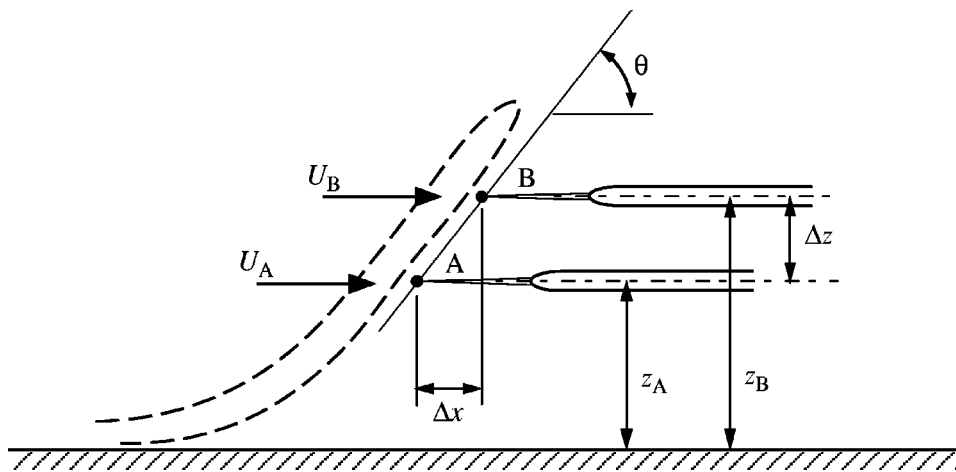


FIG. 1. Definition of terms (Ref. 32).

were reported, spanning streamwise lengths up to $2\delta_c$. For this study the experimental field-of-view was restricted to $3\delta_c$. Qualitatively, the form of the packets was similar to that observed in the channel flow simulations.

Adrian *et al.*¹⁰ emphasized that the idea of organized packets can explain many observations obtained from single point time-series measurements. This includes the sequence of multiple ejections associated with a burst event as noted by Bogard and Tiederman¹⁸ and Tardu.¹⁹ Also, streamwise packets can explain the long streamwise tail in the near-wall velocity autocorrelation function known to exist since Townsend's studies in the 1950s,⁴ and which are also well documented in other studies including those by Favre *et al.*,²⁰ Kovaszny *et al.*²¹ and Brown and Thomas.²² Similar findings are also found in experimental spectra where the wavenumber at which the peak contribution to turbulence intensity occurs corresponds to length scales five to ten times the boundary layer thickness.²³ Kim and Adrian¹³ noted similar length scales from spectra measured with hot-wires in a turbulent pipe flow. They described these structures as "very large scale motions" and speculated that these could arise from spatially correlated trains of packets. No direct evidence of this link is available as yet.

The direct evidence for packets of vortices has come from studying individual realizations of planar (experiment) and volumetric (simulation) data. In the PIV studies, typically 100 realizations were considered. Although the evidence is very suggestive, the issue remains as to whether or not packets are the statistically significant contributors to the transport phenomena in wall turbulence.

The aim of the present study is to directly investigate the link between the existence of packets of vortices to long time-averaged statistics such as the two-point velocity correlation. This is done using the framework of the attached eddy model to compute the spectra and velocity correlation functions using spatially correlated packets of hairpin vortices as the representative structures. As will be shown, the role of packets is found to be significant with its most important contribution being in the turbulent wall region (logarithmic region) of the flow.

II. TWO-POINT CORRELATIONS AND STRUCTURE ANGLE

A. Experiment

In order to define the two-point streamwise-velocity correlation as obtained in an experiment, consider the arrangement shown in Fig. 1. For streamwise velocity fluctuations (u) measured at two positions, A and B, the relevant correlation function is given by

$$\mathcal{R}_{AB} = \lim_{T \rightarrow \infty} \frac{1}{T} \int_{-T/2}^{T/2} u_A u_B dt = \overline{u_A u_B}, \quad (1)$$

where t is time, $u_A = u(x_A, 0, z_A, t)$ and $u_B = u(x_A + \Delta x, 0, z_A + \Delta z, t)$. As shown in the figure, here x is streamwise position while z is distance normal to the wall. The two-point correlation coefficient is defined as

$$R_{AB} = \frac{\overline{u_A u_B}}{\sqrt{\overline{u_A^2}} \sqrt{\overline{u_B^2}}}. \quad (2)$$

B. Attached eddy model

We wish to use the attached eddy model to calculate the equivalent velocity correlation coefficient as measured in the experiment. Only brief details of the background of the attached eddy model are presented here as detailed descriptions have been given in Refs. 6 and 8. The essential feature of the model is that it attempts to describe the kinematics of a turbulent boundary layer beyond the viscous-buffer zone by considering a statistical ensemble of coherent vortex structures. Many length scales are considered, with the range of length scales increasing with increasing Reynolds number. As will be shown in the following, quantities of interest such as spectra are calculated first for a random distribution of one scale of structure. From this, an integration across all length scales is considered with weighting functions used to account for variations in velocity scale and population density and distribution across the length scales. Given the mean velocity field and the mean momentum and continuity equations, Perry and Marusic outlined the procedure for evaluat-

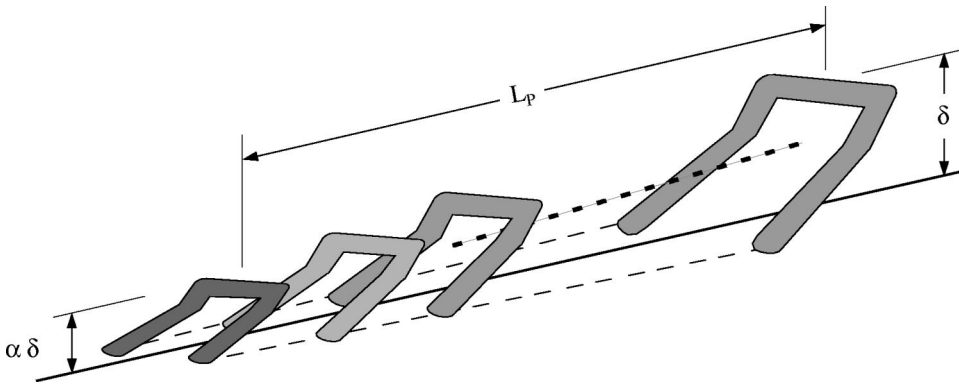


FIG. 2. Schematic of a packet of slanted Π-eddies.

ing the weighting functions. In this way the kinematic state of the flow is described (at an instance) and other turbulence statistics can then be calculated. Apart from the mean velocity field, the only direct input is the shape of the representative eddy structure.

In order to compute velocity correlations, the calculation begins by computing the induced fluctuating velocity field from one representative eddy structure and its image in the wall. Two types of representative coherent structures are being considered here, the first being individual hairpin-type structures of length scale δ , and the second being a spatially coherent packet of vortices, shown schematically in Fig. 2. Here δ is the length scale of the largest hairpin vortex in the packet. The velocity field is calculated using the Biot–Savart integral and a Gaussian distribution of vorticity is assumed in the cores of the vortices. This part of the procedure is the same as that used by Perry and Marusic.⁸ In the z_A/δ and z_B/δ planes the velocities are represented by

$$\frac{U_A^{(n)}}{U_0} = f_A\left(\frac{x}{\delta}, \frac{y}{\delta}, \frac{z_A}{\delta}\right), \tag{3}$$

$$\frac{U_B^{(n)}}{U_0} = f_B\left(\frac{x}{\delta}, \frac{y}{\delta}, \frac{z_B}{\delta}\right), \tag{4}$$

where U_0 is the velocity scale of the largest eddy in the packet, and the superscript (n) denotes the n th eddy in the packet which consists of N eddies, say, in total. If $F_A^{(n)}(k_1\delta, y/\delta, z_A/\delta)$ and $F_B^{(n)}(k_1\delta, y/\delta, z_B/\delta)$ are the Fourier transforms in the streamwise direction of f_A and f_B , respectively, then, using the shift theorem, the Fourier transforms for N eddies in the packet are

$$\psi_A\left(k_1\delta, \frac{y}{\delta}, \frac{z_A}{\delta}\right) = \frac{1}{N} \sum_{n=1}^N \left\{ F_A^{(n)}\left(k_1\delta, \frac{y}{\delta}, \frac{z_A}{\delta}\right) e^{-i2\pi k_1 X_0^{(n)}} \right\}, \tag{5}$$

$$\psi_B\left(k_1\delta, \frac{y}{\delta}, \frac{z_B}{\delta}\right) = \frac{1}{N} \sum_{n=1}^N \left\{ F_B^{(n)}\left(k_1\delta, \frac{y}{\delta}, \frac{z_B}{\delta}\right) e^{-i2\pi k_1 X_0^{(n)}} \right\}, \tag{6}$$

where k_1 is the streamwise wavenumber and $X_0^{(n)}$ is the spatial streamwise shift of the n th eddy in the packet.

The cross-power spectral density resulting from a random array of such packets over the plane (x, y) can be calculated from the spectral density function for just one packet. The result is

$$P_{AB}(k_1\delta) = \frac{U_0^2}{\lambda_x \lambda_y} \int_{-\infty}^{\infty} \psi_A^* \psi_B d\left(\frac{y}{\delta}\right), \tag{7}$$

where the asterisk indicates a complex conjugate, and λ_x and λ_y are geometric constants relating to the random distribution of packets in the $(x, y, 0)$ plane. Equation (7) is equivalent to a statement of Campbell’s theorem (see Ref. 24) for uniform density shot-noise distributions.

The total cross-power spectral density comes from integrating over the range of scales, from δ_1 , the smallest eddy length scale (assumed to be $100\nu/U_\tau$, the Kline *et al.*²⁵ scaling) to δ_c , the boundary layer thickness. That is,

$$\Phi_{AB}(k_1\delta_c) = \int_{\delta_1}^{\delta_c} P_{AB}(k_1\delta) Q^2\left(\frac{\delta}{\delta_c}\right) D\left(\frac{\delta}{\delta_c}\right) \frac{1}{\delta} d\delta, \tag{8}$$

where Q and D are weighting functions of the same type as used in the attached eddy model of Perry and Marusic.⁸ Q accounts for the variation of velocity scale for different δ ’s and D accounts for how the probability distribution function (pdf) of eddy packet scales departs from a -1 power law and how the population density on the $(x, y, 0)$ surface varies with δ .

The two-point correlation function is the inverse Fourier transform of this cross-power spectral density function. That is,

$$\mathcal{R}_{AB}(\xi) = \int_{-\infty}^{\infty} \Phi_{AB}(k_1\delta_c) e^{ik_1\delta_c\xi} d(k_1\delta_c), \tag{9}$$

where $\xi = \Delta x/\delta_c$. It is important to note that when taking the inverse Fourier transform, the full complex form of Φ_{AB} must be considered. \mathcal{R}_{AB} is guaranteed to be a purely real function since $\Phi_{AB}(-k_1\delta_c) = \Phi_{AB}^*(k_1\delta_c)$.

Finally, the two-point correlation coefficient is given by

$$R_{AB}(\xi) = \frac{\mathcal{R}_{AB}(\xi)}{\sqrt{\mathcal{R}_{AA}(0)}\sqrt{\mathcal{R}_{BB}(0)}}. \tag{10}$$

Another parameter which is often used to consider flow structure is the inferred average structure angle, or simply structure angle.²³ It is defined as the angle (θ as shown in Fig. 1) for which R_{AB} is a maximum corresponding to $\xi = \xi_m$. Therefore,

$$\theta_i = \arctan\left(\frac{\Delta z/\delta_c}{\xi_m}\right). \tag{11}$$

III. ATTACHED EDDY RESULTS

A. Single representative vortex structure

Calculations were first done by considering individual eddies as the representative structures. For the following results comparisons are made with experimental measurements made with hot-wires in a zero-pressure-gradient turbulent boundary layer at $Re_\tau=4704$ ($R_\theta=11928$). Two arrangements of hot-wires were used. The first was as shown in Fig. 1, where for a fixed Δz the wire at location B was traversed to give different Δx positions, and hence $R_{AB}(\xi)$ was mapped out one streamwise separation at a time. In the second arrangement, the wires were positioned at a fixed Δx (usually=0) and Taylor's hypothesis of frozen turbulence was used to infer ξ . Since both methods agreed, the second simpler technique was used to gather the final results which are presented here. When using Taylor's hypothesis, a fixed convection velocity of $0.82U_1$ was assumed at all levels, where U_1 is the free-stream mean velocity. Full details of the experimental facilities, procedures and experimental results are given in the thesis by Uddin²⁶ and in Ref. 27. Calculation parameters, such as $\Delta z/\delta_c$ and z_A/δ_c , were chosen to match the experimental conditions.

The first representative eddy shape to be considered is the 45° Π -eddy, shown schematically in Fig. 3(a). Marusic and Perry⁹ suggested that this simple shape may be a good candidate for the representative eddy in zero-pressure-gradient flows based on some preliminary calculations of spectra. In those calculations it was assumed for simplicity that the population density per eddy length scale follows a -1 power law and the same velocity scale is assumed per eddy length scale. Therefore, $Q^2D=1$ in Eq. (8). The same conditions are applied here.

Figures 4–6 show the results for the calculations of θ_i , R_{AA} and normalized R_{AB} respectively, throughout the layer. Figure 4 shows good agreement between experiment and calculation for the inferred average structure angle but only for approximately $z_A/\delta_c > 0.3$. The results in Figs. 5 and 6 sup-

port this conclusion with reasonably good agreement between the experiment and calculation for the correlation shapes for z_A/δ_c levels above 0.3. It is important to check the corresponding shapes of the correlation functions since θ_i depends only on the location of the peak in R_{AB} . Both the R_{AB} and R_{AA} profiles show poor agreement in the near-wall region, where the experimental results indicate that the correlations extend over $\Delta x \approx 5\delta_c$ while the Π -eddy correlations are restricted to $\Delta x \approx 1.5\delta_c$. The calculation results are perhaps expected since the largest eddy considered is of length scale δ_c and does not correlate with any other structures.

A further interesting result shown in Fig. 4 is that the structure angles computed using eddies inclined only at 45° do not necessarily give the 45° result. This is because the distribution and range of scales of eddies are also important factors influencing the result, together with vortex core effects. This makes interpretation of θ_i results difficult and this should be kept in mind when considering other studies reporting structure angle results.^{22,28–31} Figure 7 shows the calculation for only one scale of 45° Π -eddies. Here we would expect to get $\theta_i=45^\circ$ apart from any vortex core effects, and this is what the figure shows. Decreasing the core radius gives results closer to 45° . The large deviations in θ_i at high z_A/δ_c relate to probe B being in the influence of the vorticity distribution in the head of the eddy, while the lower probe A is not. This effect will change for different $\Delta z/\delta_c$. Similar results to this were also found in some earlier work reported by Perry *et al.*³²

Figures 4–6 also show the results for calculations done with a modified Π -eddy as shown in Fig. 3(b). This structure was chosen in an attempt to get lower θ_i values for $z_A/\delta_c < 0.3$. While the structure angle results do seem to agree better with experiment, compared to the 45° Π -eddies, the correlation results still are inadequate for the near-wall region, showing smaller than expected spatial correlations in the streamwise direction. It is worth noting that a shape similar to this type of hairpin vortex was inferred by Jovic³³ from

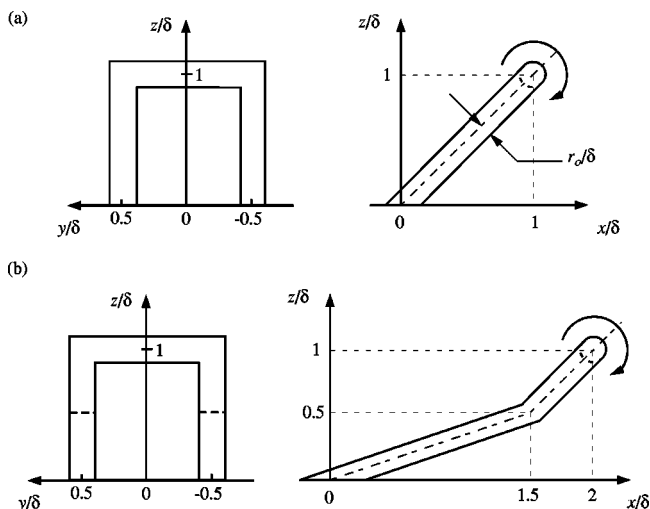


FIG. 3. Examples of simple representative attached eddies. (a) 45° Π -eddy and (b) slanted Π -eddy. A Gaussian distribution of vorticity is assumed in the cores.

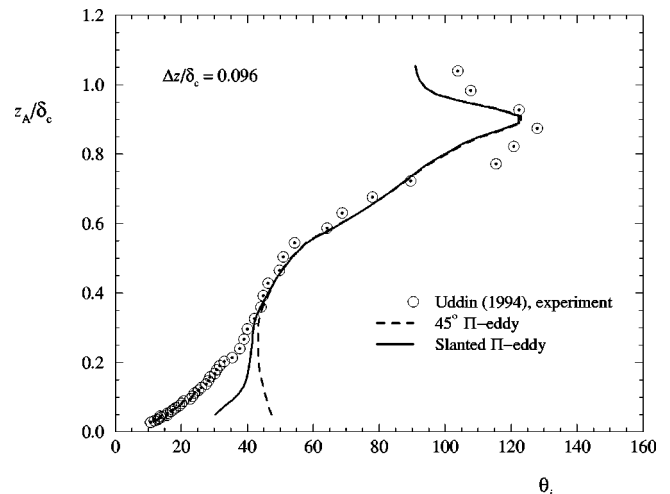


FIG. 4. Structure angles from experiment and calculated using the attached eddy model using representative eddy shapes shown in Fig. 3. Full range of length scales are considered. For both eddy shapes, $r_0/\delta=0.05$.

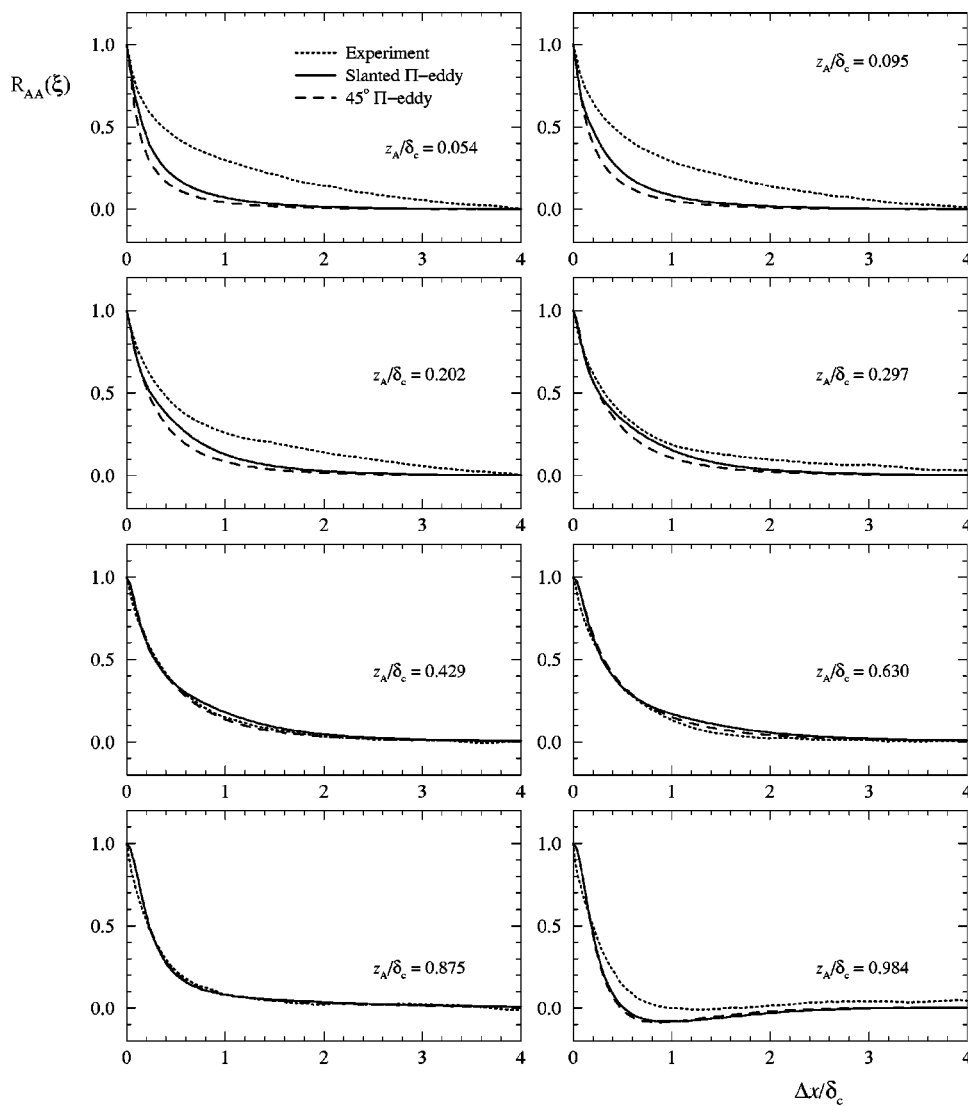


FIG. 5. Autocorrelation results at different levels through boundary layer. Dotted lines=experimental data of Ref. 26, $Re_\tau=4704$. Dashed lines=attached eddy calculation using eddy shown in Fig. 3(a). Solid line=attached eddy calculation using eddy shown in Fig. 3(b).

two-point correlation measurements in a recovering turbulent boundary layer. This shape is also very similar to the shape of individual hairpin vortices suggested by Adrian *et al.*¹⁰ based on their PIV experiments.

B. Hairpin vortex packets for near-wall region

In order to improve the prediction for the velocity correlations below approximately $z_A/\delta_c < 0.3$, many different shapes of eddies were tried, including very long streamwise individual structures. In all cases, poor agreement was found with the shape of the velocity correlation profiles and structure angle results. This leads to moving away from randomly distributed individual structures and considering an organized packet structure, of the type shown in Fig. 2. This is qualitatively similar to the structures proposed by Adrian *et al.*¹⁰ Since the single slanted Π -eddies gave reasonable results for $z_A/\delta_c \gtrsim 0.3$, a simple combination of structures is assumed. That is, for all eddy length scales $\delta > 0.35\delta_c$, the single slanted Π -eddy [Fig. 3(b)] was used as the representative shape, while a packet of slanted Π -eddies was assumed to the representative structure for $\delta \leq 0.35\delta_c$. This

implies a scenario where spatial coherence between the vortices breaks down in the outer region of the flow.

Figures 8–10 show the results for this two-part structure calculation. Very good agreement is seen for the autocorrelation and two-point correlation results and also for the structure angle. Correlation results for higher z_A/δ_c levels are not shown as they will be identical to slanted Π -eddy results shown in Figs. 5 and 6. In these calculations, the packet was made up of ten individual eddies and the largest (first) eddy was equivalent to the slanted Π -eddy shown in Fig. 3(b). All lengths of the remaining nine eddies were scaled geometrically (constant multiplication factor) such that the smallest eddy was height 0.2δ where δ is the height of the largest eddy in the packet. Therefore, following the notation in Fig. 2, $\alpha=0.2$ and the length between the smallest and largest eddy in the packet was $L_p=18\delta$. This means that the largest packet considered is of total length $6.7\delta_c$. The spatial location of each eddy in the packet was jittered, following a normal distribution, about centers corresponding to equally spaced locations between the ten eddies. The jitter is applied during the integration over y/δ in Eq. (7) for each

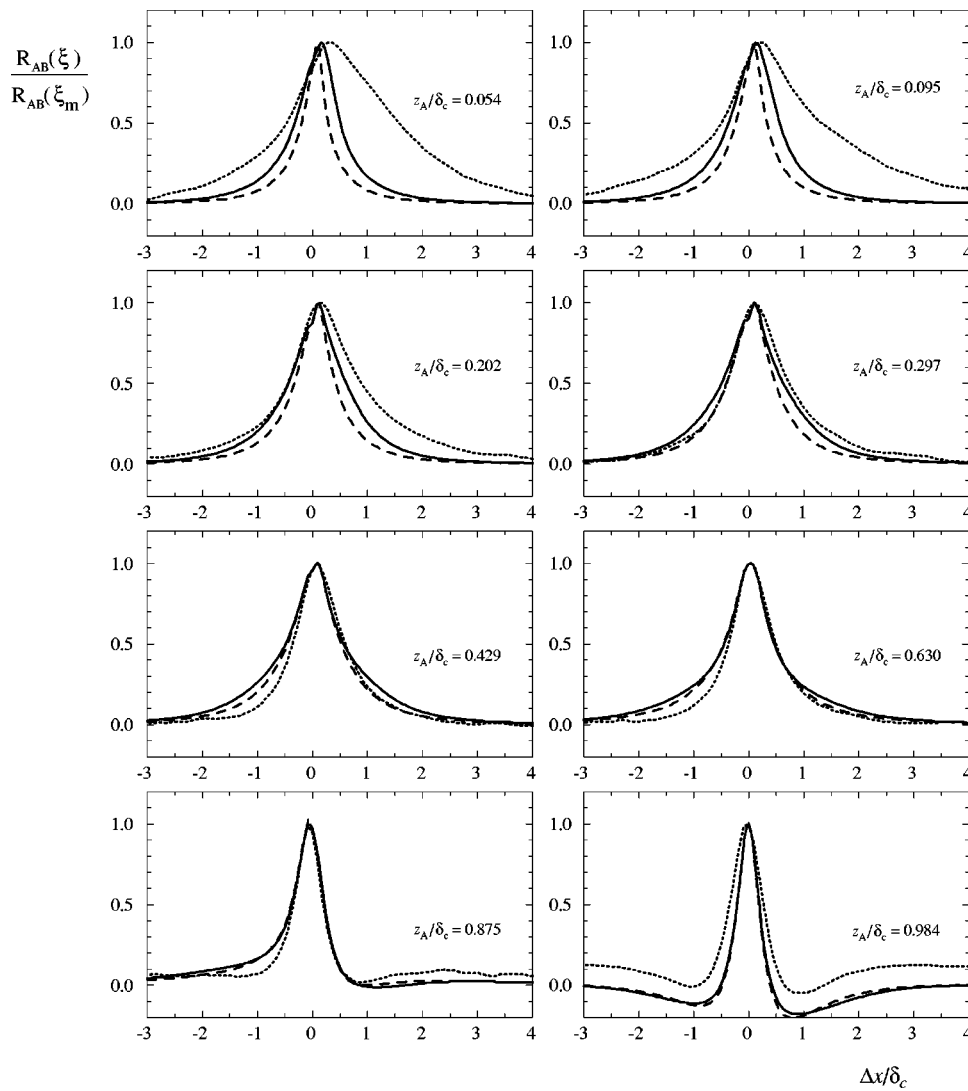


FIG. 6. Normalized two-point velocity correlations at different levels through boundary layer. For all results: $\Delta z / \delta_c = 0.096$. Dotted lines=experimental data of Ref. 26, $Re_\tau=4704$. Dashed lines=attached eddy calculation using eddy shown in Fig. 3(a). Solid line =attached eddy calculation using eddy shown in Fig. 3(b).

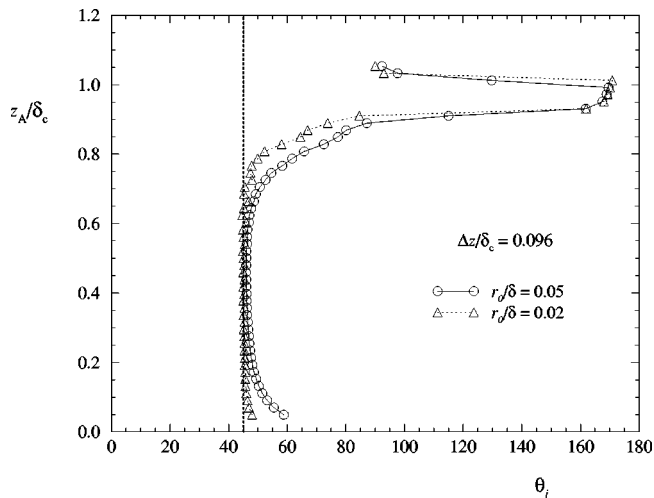


FIG. 7. Structure angles calculated using attached eddy model using only one length scale of 45° Π -eddies. Eddy shape shown in Fig. 3(a).

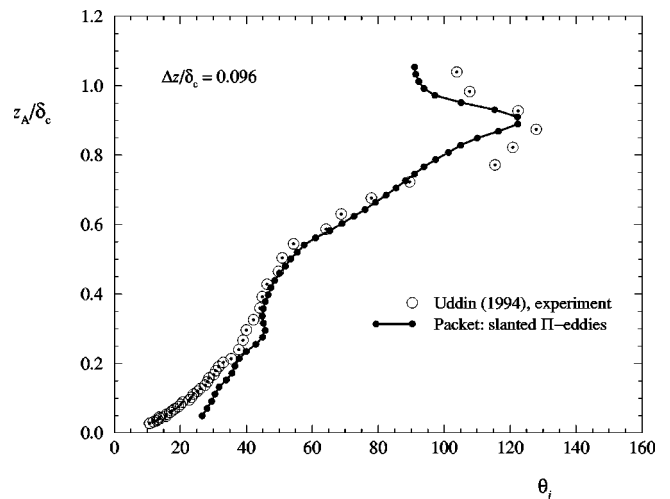


FIG. 8. Structure angles from experiment and calculated using the attached eddy model using a packet of hairpin vortices for $\delta \leq 0.35 \delta_c$ and a single hairpin [Fig. 3(b)] with $r_0 / \delta = 0.05$, for $\delta > 0.35 \delta_c$.

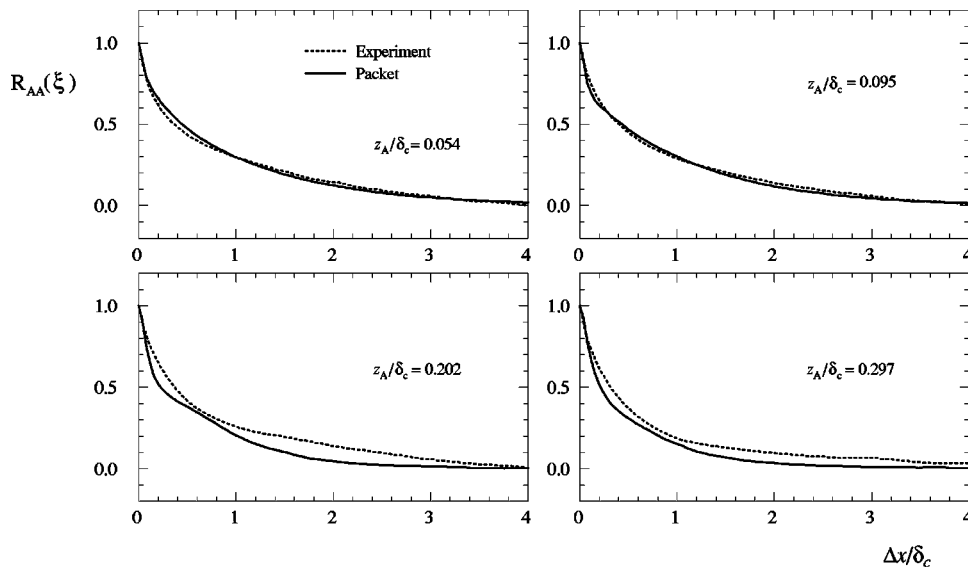


FIG. 9. As in Fig. 5, but for a packet of hairpin vortices.

δ value considered in Eq. (8). This corresponded to a discretization of 50 points for Eq. (7) and 200 points for Eq. (8). Finer discretizations showed no discernible differences in the final result.

Various combinations of L_p , number of eddies and the extent of jitter were tried. The combination described above worked best to fit the experimental data but various other combinations also gave reasonable results. For example, N could be less than 10 if more extensive jitter was applied. Therefore, no strict importance should be attached to $L_p = 18\delta$ and $N = 10$. The important feature is the organization of the eddies into a packet.

IV. DISCUSSION AND CONCLUSIONS

The approach adopted in this study follows Townsend⁴ in that different combinations of eddies are superimposed in a trial fashion, in an attempt to mimic the trends of the turbulence statistics. Here, however, the approach is more detailed through the use of the attached eddy model of Perry and Marusic.⁸ One of the difficulties in the approach of try-

ing different eddy shapes and then checking the calculation against experiment results is that there is no guarantee that the optimum solution has been found or that a unique solution exists. Therefore, to guide in the choice of structures, essentially Occam's razor has been followed. That is, the fewest possible assumptions have been made in order to explain the experimental results. Using this principle, the combination of structures chosen corresponds to having a packet of simple hairpin vortices for scales $\delta < 0.35\delta_c$, where the largest packet is approximately of size $0.35\delta_c$ in the wall-normal direction and $6.7\delta_c$ in the streamwise direction. This corresponds to packet structures spanning slightly beyond the (mean-flow) logarithmic region in the flow. In the very outer region of the flow, for length scales $\delta > 0.35\delta_c$, it is found that single hairpin vortices provide adequate results. The choice of eddy shapes that make up the packets was guided largely by the experimental results of Adrian *et al.*¹⁰

While the above organization of structures was found to be the simplest scenario that gave reasonable results, it also was the only type of organization tried that worked. It was

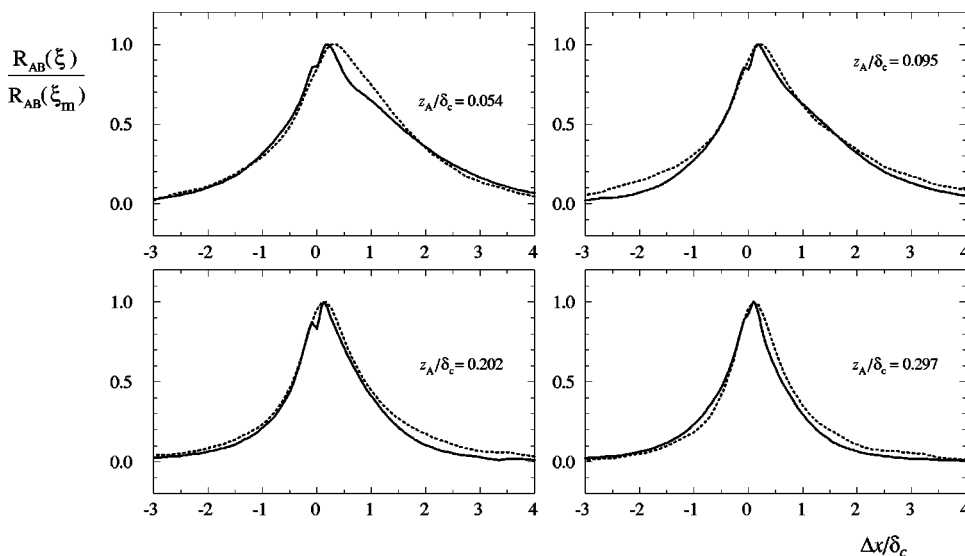


FIG. 10. As in Fig. 6, but for a packet of hairpin vortices.

clear from the study that single hairpin structures which are statistically uncorrelated with any other structures could not explain the velocity correlation trends in the logarithmic region of the flow. In addition to the single Π -eddy results presented, many different shapes were tried including very long individual structures. Townsend⁴ (pp. 156–162) also proposed a long representative eddy in the form of a double-cone. It was recognized that the main deficiency with this structure was reproducing the streamwise velocity autocorrelations. An interesting point made by Townsend was the “double-cone” could also be made up of shorter eddies of various sizes. This then is qualitatively very similar to the packet structure proposed here.

The main finding of this study is that spatially coherent packets are statistically significant structures in the logarithmic region of wall turbulence. This result supports the proposal put forward by Adrian *et al.*¹⁰ of the existence and importance of packets. It is certainly likely that refinement to the shape of both the packet structure and the single hairpin structure are required for precise matching of the Reynolds stress components and other quantities. This includes introducing outer-flow “wake” structures as described in Ref. 8. However, this would involve considerable effort and the result of this fine tuning is not expected to alter the main finding presented here.

Given the evidence that organized packets of vortices are important in near-wall transport processes, then it would seem that their role should be considered in any future modeling efforts or turbulence manipulation strategies. Further experimental study of these packet structures would be useful, including measurements such as streamwise-spanwise plane PIV to give better insight into the spatial distribution of the packets and whether any interaction between them occurs.

As a closing remark, it is perhaps worth emphasizing that the attached eddy model has been used here to identify whether or not a structural representation is feasible according to the turbulence statistics. This is where this physical model is perhaps most useful and differs from other approaches. At this stage the attached eddy model cannot be considered as a general predictive scheme as this would require information about vortex dynamics and vortex interactions which are unknown at this time. However, the studies to date have shown that an appropriate statistical distribution of vortex structures is sufficient to capture the kinematics of the boundary layer. Recently available datasets from direct numerical simulation may help provide the important information about the dynamics and work in this direction is being pursued. The present model also does not account for phenomena such as intermittency in the outer layer, as it has not been directly built in. However, this is not beyond the scope of a kinematic representation and details of how this would be done are described in Ref. 34. The modifications required are restricted to the outer-flow region and rely on similarities with the outer flow region of free turbulent shear flows. For example, Nickels and Perry³⁵ used similar concepts of assemblages of vortex structures to study turbulent coflowing jets. For the jet flow, a random array of one representative eddy of only one length scale is used and spatial

jitter is applied to the structures. This jitter is physically related to the intermittency of the outer region of the jet, with the mean position of the eddies and the amount of jitter agreeing well with experimental measurements of the turbulent/nonturbulent interface.

ACKNOWLEDGMENTS

The author wishes to thank Professor Mesbah Uddin for making available the experimental data. The support of the National Science Foundation is gratefully acknowledged, through Grant Nos. CTS-9983933 and ACI-9982274.

- ¹M. R. Head and P. Bandyopadhyay, “New aspects of turbulent structure,” *J. Fluid Mech.* **107**, 297 (1981).
- ²S. K. Robinson, “Coherent motions in turbulent boundary layers,” *Annu. Rev. Fluid Mech.* **23**, 601 (1991).
- ³R. L. Panton, *Self-Sustaining Mechanisms of Wall Turbulence* (Comp. Mech. Publications, Southampton, 1997).
- ⁴A. A. Townsend, *The Structure of Turbulent Shear Flow* (Cambridge University Press, Cambridge, 1976), Vol. 2.
- ⁵A. E. Perry and M. S. Chong, “On the mechanism of wall turbulence,” *J. Fluid Mech.* **119**, 173 (1982).
- ⁶A. E. Perry, S. M. Henbest, and M. S. Chong, “A theoretical and experimental study of wall turbulence,” *J. Fluid Mech.* **165**, 163 (1986).
- ⁷A. A. Townsend, *The Structure of Turbulent Shear Flow* (Cambridge University Press, Cambridge, 1956).
- ⁸A. E. Perry and I. Marusic, “A wall-wake model for the turbulence structure of boundary layers. Part 1. Extension of the attached eddy hypothesis,” *J. Fluid Mech.* **298**, 361 (1995).
- ⁹I. Marusic and A. E. Perry, “A wall-wake model for the turbulence structure of boundary layers. Part 2. Further experimental support,” *J. Fluid Mech.* **298**, 389 (1995).
- ¹⁰R. J. Adrian, C. D. Meinhart, and C. D. Tomkins, “Vortex organization in the outer region of the turbulent boundary layer,” *J. Fluid Mech.* **422**, 1 (2000).
- ¹¹J. Zhou, C. D. Meinhart, S. Balachandar, and R. J. Adrian, “Formation of coherent hairpin packets in wall turbulence,” in *Self-Sustaining Mechanisms of Wall Turbulence*, edited by R. L. Panton (Comp. Mech. Publications, Southampton, 1997).
- ¹²C. D. Meinhart and R. J. Adrian, “On the existence of uniform momentum zones in a turbulent boundary layer,” *Phys. Fluids* **7**, 694 (1995).
- ¹³K. C. Kim and R. J. Adrian, “Very large-scale motion in the outer layer,” *Phys. Fluids* **11**, 417 (1999).
- ¹⁴J. Zhou, R. J. Adrian, S. Balachandar, and T. M. Kendall, “Mechanisms for generating coherent packets of hairpin vortices in channel flow,” *J. Fluid Mech.* **387**, 353 (1999).
- ¹⁵J. Zhou, R. J. Adrian, and S. Balachandar, “Autogeneration of near wall vortical structure in channel flow,” *Phys. Fluids* **8**, 288 (1996).
- ¹⁶Z. C. Liu and R. J. Adrian, “Evidence for hairpin packet structure in DNS channel flow,” in *Proc. Turb. Shear Flow Phen. 1*, Santa Barbara, CA, 1999.
- ¹⁷C. R. Smith, J. D. A. Walker, A. H. Haidari, and U. Soburn, “On the dynamics of near-wall turbulence,” *Philos. Trans. R. Soc. London, Ser. A* **336**, 131 (1991).
- ¹⁸D. G. Bogar and W. G. Tiederman, “Burst detection with single-point velocity measurements,” *J. Fluid Mech.* **162**, 389 (1986).
- ¹⁹S. Tardu, “Characteristics of single and clusters of bursting events in the inner layer, Part 1: Vita events,” *Exp. Fluids* **20**, 112 (1995).
- ²⁰A. J. Favre, J. J. Gaviglio, and R. J. Dumas, “Space-time double correlations and spectra in a turbulent boundary layer,” *J. Fluid Mech.* **2**, 313 (1957).
- ²¹L. S. G. Kovaszny, V. Kibens, and R. F. Blackwelder, “Large-scale motion in the intermittent region of a turbulent boundary layer,” *J. Fluid Mech.* **41**, 283 (1970).
- ²²G. R. Brown and A. S. W. Thomas, “Large structure in a turbulent boundary layer,” *Phys. Fluids* **20**, S243 (1977).
- ²³A. J. Smits and J. P. Dussauge, *Turbulent Shear Layers in Supersonic Flow* (AIP, Woodbury, NY, 1996).
- ²⁴A. Papoulis, *Probability, Random Variables and Stochastic Processes* (McGraw-Hill, New York, 1965).
- ²⁵S. J. Kline, W. C. Reynolds, F. A. Schaub, and P. W. Rundstadler, “The

- structure of turbulent boundary layers," J. Fluid Mech. **30**, 741 (1967).
- ²⁶A. K. M. Uddin, "The structure of a turbulent boundary layer," Ph.D. thesis, University of Melbourne, Australia, 1994.
- ²⁷I. Marusic and A. K. M. Uddin, "A study of organized motions in turbulent boundary layers" (in preparation).
- ²⁸A. E. Alving, A. J. Smits, and J. H. Wamuff, "Correlation measurements and structure angles in a turbulent boundary layer recovering from convex curvature," J. Fluid Mech. **211**, 529 (1990).
- ²⁹P. MacAulay and I. P. Gartshore, "A tentative model of outer-region structure in a turbulent boundary layer developing on a smooth wall," in *Experimental Heat Transfer, Fluid Mechanics and Thermodynamics 1991*, edited by J. F. Keffer, R. K. Shah, and E. N. Ganic (Elsevier Science, Amsterdam, 1991).
- ³⁰E. F. Spina and A. J. Smits, "Organized structures in a compressible turbulent boundary layer," J. Fluid Mech. **182**, 85 (1987).
- ³¹J. P. Dussauge, H. Fernholz, P. J. Finley, R. W. Smith, A. J. Smits, and E. F. Spina, "Turbulent boundary layers in subsonic and supersonic flow," AGARDograph 335 (1996).
- ³²A. E. Perry, A. K. M. Uddin, and I. Marusic, "Similarity laws and attached eddy shapes in turbulent boundary layers," in *Proc. 12th Australasian Fluid Mechanics Conference*, Sydney, Australia, 1995.
- ³³S. Jovic, "Two-point correlation measurements in a recovering turbulent boundary layer, in *Near-Wall Turbulent Flows*, edited by R. M. C. So, C. G. Speziale, and B. E. Launder (Elsevier Science, Amsterdam, 1993).
- ³⁴T. B. Nickels and I. Marusic, "On some differences in the structure of turbulent jets and boundary layers," J. Fluid Mech. (submitted).
- ³⁵T. B. Nickels and A. E. Perry, "An experimental and theoretical study of the turbulent coflowing jet," J. Fluid Mech. **309**, 157 (1996).